

This article was downloaded by:

On: 14 January 2011

Access details: *Access Details: Free Access*

Publisher *Taylor & Francis*

Informa Ltd Registered in England and Wales Registered Number: 1072954 Registered office: Mortimer House, 37-41 Mortimer Street, London W1T 3JH, UK



Molecular Simulation

Publication details, including instructions for authors and subscription information:

<http://www.informaworld.com/smpp/title~content=t713644482>

Electronic Structure Calculations of High T_c Materials

W. M. Temmerman^a; P. A. Sterne^a; G. Y. Guo^a; Z. Szotek^a

^a SERC Daresbury Laboratory, Warrington, UK

To cite this Article Temmerman, W. M. , Sterne, P. A. , Guo, G. Y. and Szotek, Z.(1989) 'Electronic Structure Calculations of High T_c Materials', *Molecular Simulation*, 4: 1, 153 – 164

To link to this Article: DOI: 10.1080/08927028908021971

URL: <http://dx.doi.org/10.1080/08927028908021971>

PLEASE SCROLL DOWN FOR ARTICLE

Full terms and conditions of use: <http://www.informaworld.com/terms-and-conditions-of-access.pdf>

This article may be used for research, teaching and private study purposes. Any substantial or systematic reproduction, re-distribution, re-selling, loan or sub-licensing, systematic supply or distribution in any form to anyone is expressly forbidden.

The publisher does not give any warranty express or implied or make any representation that the contents will be complete or accurate or up to date. The accuracy of any instructions, formulae and drug doses should be independently verified with primary sources. The publisher shall not be liable for any loss, actions, claims, proceedings, demand or costs or damages whatsoever or howsoever caused arising directly or indirectly in connection with or arising out of the use of this material.

ELECTRONIC STRUCTURE CALCULATIONS OF HIGH T_c MATERIALS

W.M. TEMMERMAN, P.A. STERNE, G.Y. GUO and Z. SZOTEK

SERC Daresbury Laboratory, Warrington WA4 4AD, UK

(Received January 1989, accepted February 1989)

We outline the computational methods used to perform accurate and reliable LMTO-ASA (Linear Muffin-Tin Orbitals in the Atomic Sphere Approximation) calculations within the LDA (Local Density Approximation) or LSD (Local Spin Density). In particular we discuss the evaluation of Brillouin zone integrals, reconstruction of the electronic charge densities, evaluation of the total energy and convergence of the self-consistent-field cycles. We also elaborate on how the LMTO-ASA code makes use of the vector and parallel aspects of the new computer architectures. Finally, we present results of antiferromagnetic calculations for La_2CuO_4 , La_2NiO_4 and $\text{YBa}_2\text{Cu}_3\text{O}_6$.

KEY WORDS: Electronic structure, high T_c , muffin-tin, local density approximate, local spin density

1. INTRODUCTION

The quantum mechanical study of the electronic structure of solids is usually performed in a mean field way either through a Hartree-Fock (HF) approach or Density Functional Theory (DFT). In contrast, the successful application of Configuration Interaction type of approaches is only limited to molecular and fully ionic crystals. The HF and DFT differ in their treatment of the exchange and correlation. HF incorporates the exchange exactly and has various schemes to include correlation effects. The DFT on the other hand treats both the exchange and correlation on equal footing but in an approximate way. From a computational point of view the DFT in its various approximations such as LDA (Local Density Approximation) and LSD (Local Spin Density) is easier to implement for complicated systems since it leads to local potentials. However there have been some recent implementations of the HF method for complex crystalline systems [1]. This article describes how to perform reliable and accurate self-consistent field (SCF) LDA/LSD electronic structure calculations for complex solids with the linear muffin-tin orbitals atomic sphere approximation method (LMTO-ASA). As an example of this we will discuss our work on antiferro magnetism in high T_c materials.

The outline of the paper is as follows: the second section gives a brief introduction into the LMTO-ASA band structure method. The third section contains the important ingredients necessary to have a reliable and accurate LMTO-ASA code for complicated systems. The fourth section contains our results of antiferromagnetic band structure studies of La_2CuO_4 , $\text{YBa}_2\text{Cu}_3\text{O}_6$ and La_2NiO_4 . Section 5 has our conclusions.

2. THE LMTO-ASA BAND STRUCTURE METHOD

The foundations of DFT are two theorems due to Hohenberg and Kohn (HK) [2]. They can be stated as follows (in atomic units):

$$H = T + U + V = \sum_{i=1}^N (-\nabla_i^2) + \frac{1}{2} \sum_{i \neq j}^N \sum_{j=1}^N \frac{2}{r_{ij}} + \sum_{i=1}^N v_{\text{ext}}(\mathbf{r}_i) \quad (1)$$

where H is the Hamiltonian of a system of N interacting electrons, T their kinetic energy, U the electron-electron Coulomb repulsion and V some external potential, for example the Coulomb attraction of the nuclei. First HK showed that the external potential is a unique functional of the electron density $\mu(\mathbf{r})$, and hence the properties of the groundstate Φ of an inhomogeneous interacting electron gas are unique functionals of the electron density. Second, they showed that $\langle \Phi | H | \Phi \rangle = E[\mu]$ is a minimum for the true electron density. Kohn and Sham [3] then showed that this minimization leads to N effective single-particle Schrödinger equations:

$$(-\nabla^2 + V(\mathbf{r}) - \varepsilon_i) \psi_i(\mathbf{r}) = 0$$

$$\rho(\mathbf{r}) = \sum_i |\psi_i(\mathbf{r})|^2 \theta(\varepsilon_F - \varepsilon_i) \quad (2)$$

$$V(\mathbf{r}) = 2 \int d\mathbf{r}' \frac{\rho(\mathbf{r}')}{|\mathbf{r} - \mathbf{r}'|} + \frac{\delta E_{\text{xc}}[\rho]}{\delta \rho(\mathbf{r})} + v_{\text{ext}}(\mathbf{r}) \quad (3)$$

$E_{\text{xc}}[\rho]$ is the unknown exchange and correlation functional of the charge density. In the local density approximation one writes:

$$E_{\text{xc}}[\rho] \approx \int d^3\mathbf{r} \rho(\mathbf{r}) \varepsilon_{\text{xc}}^{(\text{h})}(\rho(\mathbf{r})) \quad (4)$$

where $\varepsilon_{\text{xc}}^{(\text{h})}(x)$ is the contribution of exchange and correlation to the total energy (per electron) in a homogeneous, but interacting, electron gas of density $\rho(\mathbf{r})$. This quantity $\varepsilon_{\text{xc}}^{(\text{h})}$ [21] can be determined to sufficient accuracy.

It follows then that in solids, Equation (2), which is a set of self-consistent equations in the charge density, has to be solved for a periodic arrangement of external potentials. This can be simplified by making use of the lattice periodicity. However, this still leaves us with a formidable numerical problem which we will further simplify by assuming that the potential $V(\mathbf{r})$ is spherically symmetric within overlapping Wigner-Seitz spheres. This is the so-called atomic sphere approximation or ASA [4, 5].

If we then choose a linear combination of the solutions ϕ of the radial Schrödinger equation in the ASA, which are called the muffin-tin orbitals, and their energy derivative $\dot{\phi}$ in an expansion of the wavefunction, then application of the variational principle leads to the following generalised eigenvalue problem for the energy eigenvalues $\varepsilon_{\mathbf{k},n}$ and wavefunctions $\Psi_{\mathbf{k},n}$, where \mathbf{k} refers to the \mathbf{k} point in reciprocal space and n the band index:

$$(H_{\text{LL}}^{\mathbf{k}} - \varepsilon_{\mathbf{k},n} O_{\text{LL}}^{\mathbf{k}}) \mathbf{a}_{\text{L}}^{\mathbf{k},n} = 0$$

and

$$\psi_{\mathbf{k},n}(\mathbf{r}) = \sum_{i,\text{L}} [A_{\text{L}}^{\mathbf{k},n}(\varepsilon_{\mathbf{k},n}) \phi_{i,\text{L}}^{\mathbf{k}}(\mathbf{r}) + B_{\text{L}}^{\mathbf{k},n}(\varepsilon_{\mathbf{k},n}) \dot{\phi}_{i,\text{L}}^{\mathbf{k}}(\mathbf{r})] Y_{\text{L}}(\mathbf{r}) \quad (5)$$

The indices L and L' are the angular momenta quantum numbers l, m . The index i sums over the different atomic spheres which make up the unit cell. The Y 's are the spherical harmonics, $\phi_{v,L}^i$ is the solution of the radial Schrödinger equation in ASA i , energy E_v and angular momentum l , $\dot{\phi}$ is the energy derivative of ϕ . For the detailed form of the Hamiltonian H , the overlap matrix O and wavefunction coefficients A and B we refer the reader to formulae (5.46), (5.47) and (6.30) of Skriver's book [5].

The advantage of this particular basis set method is that the matrices are small. Because of the ASA, the matrix elements of H and O are analytical functions of the logarithmic derivatives of a single atomic sphere wavefunction, ϕ , and the solid state effects enter through the structure constants which depend only on the crystal structure. We note that the basis functions ϕ and $\dot{\phi}$ in (5) are independent of principal quantum number n . In circumstances where one wants to generate the band structure over an energy range which would include bands of different principal quantum number, such as is the case for the calculation of occupied and unoccupied band structures, one should include in the basis set the basis function of corresponding to these different n . The size of the generalised eigenvalue problem then scales according to the number of principal quantum numbers included. In that case one might consider a non-linear band structure approach, such as the KKR and APW partial wave methods. In these methods the matrix size remains constant, but they have a complicated non-linear energy dependence and the eigenvalues are obtained by finding the zeroes of the determinant of the KKR or APW matrices.

3. ON THE LMTO-ASA CODE

Figure 1 gives a flowchart of the SCF-LMTO-ASA code. We will discuss the features of the calculation which we found very important in obtaining an accurate and reliable code. One starts with an input V^{in} , usually obtained from atomic charge densities which are suitably normalised over the atomic sphere. Given this input potential the generalised eigenvalue problem (a in Figure 1) is solved via standard numerical techniques (such as Cholesky decomposition) and codes (the EISPACK routines: HTRIDI, IMTQL2 and HTRIBK). This is an adequate procedure for the matrix sizes we are dealing with (of the order of 100). In step b of Figure 1 we collect all the energy eigenvalues and vectors for a summation over the Brillouin zone (k sum) and over band indices (n sum) to determine the charge density. To perform the k sum the irreducible Brillouin zone wedge is divided in tetrahedra. At the vertices of these tetrahedra the energy eigenvalues and vectors are calculated. On the basis of a linear variation of the energy eigenvalues over the tetrahedron [6, 7] analytical expressions for the contributions of a particular tetrahedron to the density of states and integrated density of states can be obtained and are given in Table 1. One can derive expressions for the higher energy moments of the density of states: we determined expressions for up to the third moment with the help of the algebraic manipulation package REDUCE. Out of the value I_1^e from Table 1 we can define weight W as follows:

$$W_{k_j, n} = \sum_{\text{tet}} \sum_{i=1}^4 I_{k_i, n}^{\text{ef}} \delta(k_i - k_j).$$

The first summation is over all the tetrahedra spanning the irreducible wedge of the Brillouin zone and the second summation is over the four vertices of each tetrahedron. The Brillouin zone integrals of the wavefunction coefficient then become the following k sums:

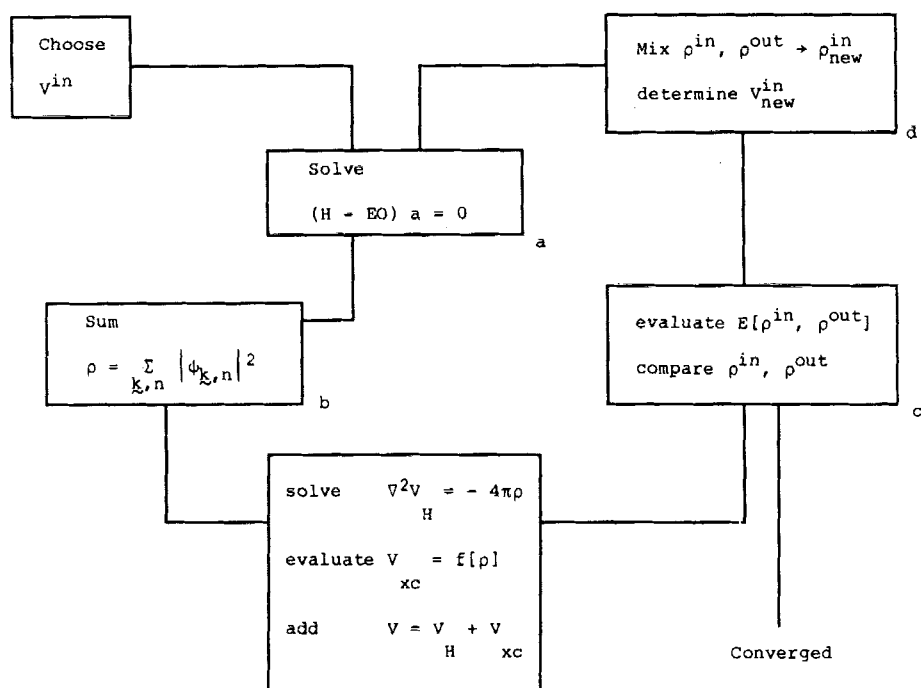


Figure 1 Flowchart of the SCF-LMTO-ASA program.

$$A_L = \sum_n \sum_{k_j} A_L^{k_j, n} W_{k_j, n}$$

$$B_L = \sum_n \sum_{k_j} B_L^{k_j, n} W_{k_j, n}$$

The charge density for the i^{th} site in the unit cell then becomes:

$$\begin{aligned} \varrho^i(\mathbf{r}) = & \sum_L [|A_L|^2 (\phi_{v,L}^i(\mathbf{r}))^2 + |B_L|^2 \\ & \times (\phi_{v,L}^i(\mathbf{r}))^2 + (A_L^* B_L + B_L^* A_L) \phi_{v,L}^i(\mathbf{r}) \dot{\phi}_{v,L}^i(\mathbf{r})] \end{aligned}$$

An alternative method of calculating the charge density via a moment expansion of the density of states (expression (6.41) in Skriver's book [51]) was found to give a substantial slower convergence of at least twice as many SCF cycles. This is because expression (6.41) does not span the Hilbert space defined by ϕ and $\dot{\phi}$.

One of the most important ingredients in the rate of convergence is the mixing scheme to obtain from the output charge density ϱ^{out} a new input charge density $\varrho_{\text{new}}^{\text{in}}$ [step c in Figure 1]. A vast literature on the subject exists and an excellent review of the various methods is given by Pickett [8]. We found it adequate to implement a generalization of a simple linear mixing due to Anderson [9]. This scheme uses a linear combination of input and output densities of two successive iterations (M-1 and M) to give an optimized input $\bar{\varrho}^{\text{in}}$ and output $\bar{\varrho}^{\text{out}}$:

Table 1 The analytical expressions for the contributions of a particular tetrahedron, defined by E_1, E_2, E_3, E_4 as energy eigenvalues with the same band index at k points 1 2 3 4 which define a tetrahedron, to the density of states and integrated density of states.

<i>Density of states</i>		<i>Integrated density of states</i> $\int_{-\infty}^E n(E') dE'$	
$n_1 = \frac{3^*(E - E_1)^2}{(E_2 - E_1)(E_3 - E_1)(E_4 - E_1)} \theta(E - E_1)$		$I_1 = \frac{(E - E_1)^3}{(E_2 - E_1)(E_3 - E_1)(E_4 - E_1)} \theta(E - E_1)$	
$n_2 = \frac{3^*(E - E_2)^2}{(E_1 - E_2)(E_3 - E_2)(E_4 - E_2)} \theta(E - E_2)$		$I_2 = \frac{(E - E_2)^3}{(E_1 - E_2)(E_3 - E_2)(E_4 - E_2)} \theta(E - E_2)$	
$n_3 = \frac{3^*(E - E_3)^2}{(E_1 - E_3)(E_2 - E_3)(E_4 - E_3)} \theta(E - E_3)$		$I_3 = \frac{(E - E_3)^3}{(E_1 - E_3)(E_2 - E_3)(E_4 - E_3)} \theta(E - E_3)$	
$n_4 = \frac{3^*(E - E_4)^2}{(E_1 - E_4)(E_2 - E_4)(E_3 - E_4)} \theta(E - E_4)$		$I_4 = \frac{(E - E_4)^3}{(E_1 - E_4)(E_2 - E_4)(E_3 - E_4)} \theta(E - E_4)$	
$E \leq E_1$	0	$E \leq E_1$	0
$E_1 \leq E < E_2$	n_1	$E_1 \leq E < E_2$	I_1
$E_2 \leq E < E_3$	$n_1 + n_2$	$E_2 \leq E < E_3$	$I_1 + I_2$
$E_3 \leq E < E_4$	$n_1 + n_2 + n_3$	$E_3 \leq E < E_4$	$I_1 + I_2 + I_3$
$E_4 \leq E$	$n_1 + n_2 + n_3 + n_4 = 0$	$E_4 \leq E$	$I_1 + I_2 + I_3 + I_4 = I$

$$\bar{\varrho}_M^{\text{in(out)}} = \theta_M \varrho_M^{\text{in(out)}} + (1 - \theta_M) \varrho_{M-1}^{\text{in(out)}}$$

and θ_M is determined by minimizing the distance Δ

$$\Delta(\mathbf{r}) = (\varrho^{\text{out}}(\mathbf{r}) - \varrho^{\text{in}}(\mathbf{r}))$$

between $\bar{\varrho}_M^{\text{out}}$ and $\bar{\varrho}_M^{\text{in}}$ (i.e. convergence is obtained when $\bar{\varrho}_M^{\text{out}} = \bar{\varrho}_M^{\text{in}}$) which leads to the following expression for θ_M :

$$\theta_M = \frac{\int d\mathbf{r} [\Delta_{M-1}(\mathbf{r}) \Delta_{M-1}(\mathbf{r}) - \Delta_{M-1}(\mathbf{r}) \Delta_M(\mathbf{r})]}{\int d\mathbf{r} [\Delta_M(\mathbf{r}) - \Delta_{M-1}(\mathbf{r})]^2}$$

The new input charge density is then obtained from

$$\varrho_{M+1}^{\text{in}} = \lambda \bar{\varrho}_M^{\text{out}} + (1 - \lambda) \bar{\varrho}_M^{\text{in}}$$

where we treat λ like the mixing parameter in the simple linear mixing scheme. More sophisticated mixing methods are available such as Broyden's method [10].

The quantity which converges first should be the total energy since the functional $E_{\text{total}}[\varrho]$ is minimized by the true ground state density $\varrho(\mathbf{r})$. However care has to be taken by using a total energy expression which is truly variational. This is especially the case when using a total energy expression which incorporates the one-electron sum which is not a functional of either the input or output density alone [11, 18]. The LMTO-ASA variational total energy expressions are:

$$\begin{aligned} E = & \int \varepsilon n(\varepsilon) d\varepsilon - \int V_H^n \varrho^{\text{out}} d\mathbf{r} + \frac{1}{2} \int V_H^{\text{out}} \varrho^{\text{out}} d\mathbf{r} - \int \mu_{\text{xc}}[\varrho^{\text{in}}] \varrho^{\text{out}} d\mathbf{r} \\ & + \int \varepsilon_{\text{xc}}[\varrho^{\text{out}}] \varrho^{\text{out}} d\mathbf{r} + \int [\varepsilon_{\text{xc}}[\varrho^{\text{out}}] - \varepsilon_{\text{xc}}[\varrho_{\text{core}}]] \varrho_{\text{core}} d\mathbf{r} + E_{\text{MAD}} \\ E_{\text{MAD}} = & \frac{1}{\zeta_{\text{av}}} \left[\frac{1}{2} Z_{\text{ion}}^i V_{\text{MAD}}^{ij} Z_{\text{ion}}^j + \frac{1}{2} q_{\text{val}}^{\text{out},i} V_{\text{MAD}}^{ij} q_{\text{val}}^{\text{out},j} - q_{\text{val}}^{\text{in},i} V_{\text{MAD}}^{ij} q_{\text{val}}^{\text{out},j} \right] \end{aligned}$$

where Z and q are respectively the charge of ion core and the electronic charge of the valence electrons. We also made use of an analytical expression for the first moment of the density of states or the one-electron sum.

In summary, we obtain a fast and reliable convergence within the LMTO-ASA scheme by making use of analytical expressions, derived within the linear tetrahedra method, for the Brillouin zone integrals, evaluating the charge density from the wavefunctions, a better than linear mixing scheme and finally by evaluating the variational expression of the total energy.

4. APPLICATION: ANTIFERROMAGNETISM IN HIGH T_c MATERIALS

The parent compounds of the high T_c materials are antiferromagnetic insulators. Doping, either through substitution on the La metal sublattice or through stoichiometry on the O sublattice makes these materials high T_c superconductors [12, 13]. There is experimental evidence that upon doping O holes are created [14]. What is presently under debate is whether the O holes are of $dp \sigma$ or $dp \pi$ character and whether their symmetry is p_{xy} or p_z or a mixture [15].

In Figure 2 we show the density of states of La_2CuO_4 in the orthorhombic structure (space group Cmca or Bmba) decomposed according to symmetry and site. We note

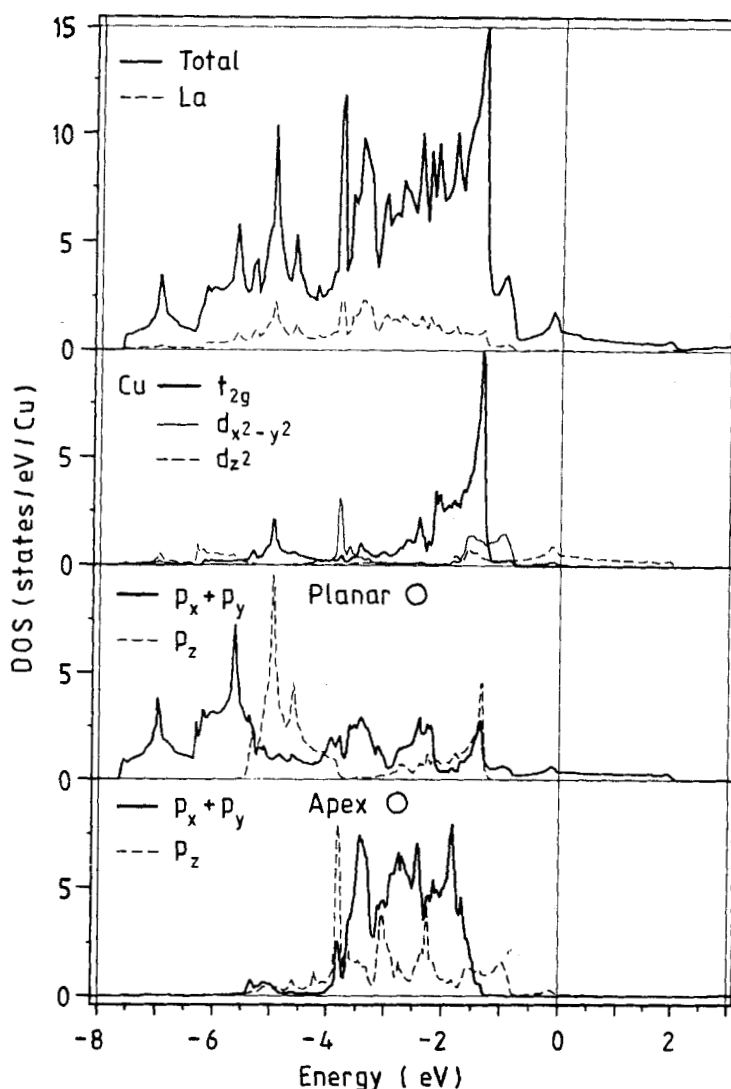


Figure 2 Total density of states, and its site and symmetry decomposition in body-centred tetragonal La_2CuO_4 .

from these densities of states the very strong hybridization of the Cu d bands with the O p bands, giving rise to a bandwidth of 9 eV. Because of the substantial distortion of the CuO_6 octahedra, a $\text{Cu-O}_{\text{planar}}$ bondlength of 1.89 Å and a $\text{Cu-O}_{\text{apex}}$ bondlength of 2.42 Å, there is a big difference in the densities of states of the planar O and the apex O and also of the Cu t_{2g} and e_g orbitals. We find the Cu t_{2g} orbitals more localised around a peak at -1.4 eV binding energy than the e_g orbitals which extend over a bigger energy range. The hybridizing Cu $d_{x^2-y^2}$ and the planar $\text{O}p_{x,y}$ are the only orbitals contributing substantially at ϵ_F , and these are the orbitals which give rise to

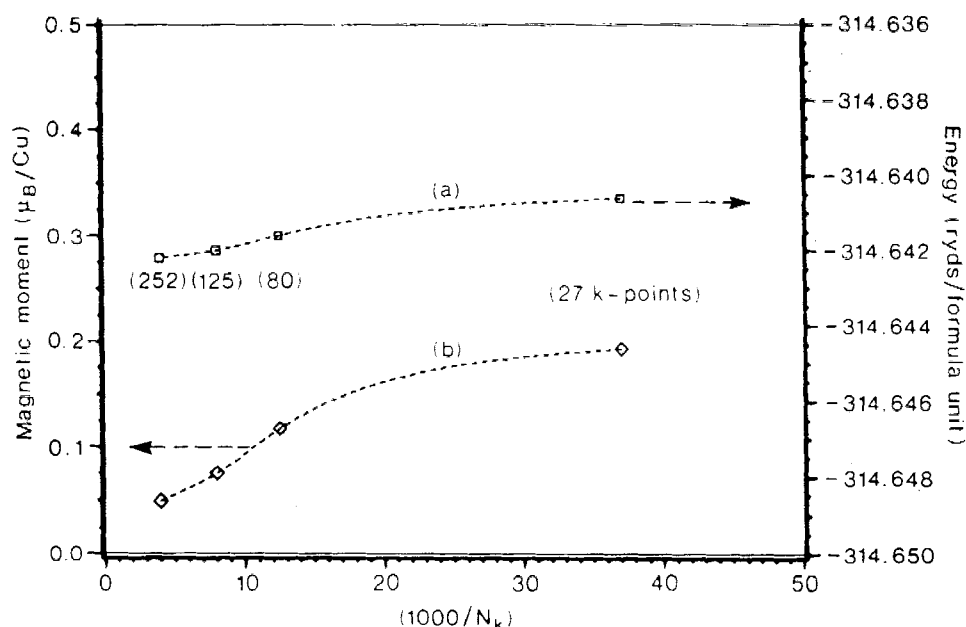


Figure 3 The self-consistent antiferromagnetic moment on each Cu site (a), and total energy (b), versus the number of k points inside the irreducible $1/8$ of the Brillouin zone of the body-centred orthorhombic La_2CuO_4 . The lines are merely a guide to the eye.

the 9 eV bandwidth. The Cu d_{z^2} orbitals hybridise with the apex $\text{O}p_z$ bands and are occupied with no contributions at ϵ_F . The apex $\text{O}p_{x,y}$ is essentially non-bonding and extends from -1.7 eV to -4 eV. The planar $\text{O}p_z$ band is split into two by its interaction with Cu t_{2g} bands: one peak at -4.7 eV, the other one at -1.4 eV. The La bands hybridise over the whole band width in their role as electron donors.

The LSD calculations fail to describe La_2CuO_4 [16, 17] and $\text{YBa}_2\text{Cu}_3\text{O}_6$ [18] as antiferromagnetic insulators. Even though the Fermi energy lies in the middle of an

Table 2 Total energy and its decompositions of the base-centred orthorhombic La_2CuO_4 in the non-magnetic and antiferromagnetic states, calculated using 80 k-points inside the irreducible Brillouin Zone wedge in the Brillouin Zone integration.

Mag. state	E_{tot} (Ryds)	E_{band} (Ryds)	E_{Cu} (Ryds)	E_{L} (Ryds)	Mag. moment (μ_B/Cu)
(a) non-mag.	-314.641	-46.452	-76.619	-191.570	0.0
(b) AF	-314.642	-46.455	-76.619	-191.568	0.117 ^a
(c) AF (non-SC)	-314.632	-46.731	-76.681	-191.220	0.348 ^b

^a It reduces to the negligibly small value when more k-points are included in the Brillouin Zone integration (see fig. 3)

^b Non self-consistent moment, see text.

anti-bonding $\text{Cu } d_{x^2-y^2}$ O $p_{x,y}$ band, a Peierls gap does not open up when allowing for an antiferromagnetic ordering between the neighbouring Cu spins in the [110] direction. The convergence of the total energy as a function of the number of k-points is readily established as can be seen from Figure 3. However whether there will be a residual small magnetic moment or no moment at all could not be decided from this figure. In Table 2 we compare the various contributions to the total energy. From this we see the competition between E_{Coulomb} on the one hand and E_{xc} and E_{band} on the other. By either increasing E_{Coulomb} or increasing $E_{\text{xc}} + E_{\text{band}}$ an antiferromagnetic insulator could be obtained. Whilst the common wisdom seems to be that LSD calculations under-estimate E_{xc} [16, 17], we discussed in [18] the strong dependence of the electronic and magnetic properties on the charges in the Cu and O spheres, i.e. E_{Coulomb} . Therefore the problem could as likely be an under-estimation of E_{Coulomb} .

The tendency towards magnetism can usually be enhanced by expanding the lattice. The reasoning behind this is that the magnitude of the U/W ratio, where U is the on-site Coulomb interaction and W the bandwidth, determines the magnetic properties. Whilst U is predominantly an atomic quantity, hardly affected by its solid state surroundings, W can be decreased by expanding the lattice. By performing calculations for La_2CuO_4 on an expanded lattice (and also a contracted lattice) we could not find any substantial change in the magnetic moment [18]. This surprising result, together with our observation that the magnetic properties were more sensitive to the charges on the Cu and O spheres, made us turn to study the magnetic properties of La_2NiO_4 which has the same structure as La_2CuO_4 .

In La_2NiO_4 , the strong hybridization of the metal (Cu) and oxygen bands does not occur, and the Ni d band is separated from the O p band, with the O p band at higher binding energy [19]. The Fermi energy crosses both the Ni $d_{x^2-y^2}$ and d_{z^2} bands. For La_2NiO_4 the antiferromagnetic state is the ground state with a moment of $0.7 \mu_B$. On expanding the lattice this moment saturates to $1.2 \mu_B$ (Table 3).

Whilst this behaviour on expanding La_2NiO_4 is what one would have expected, we find also that by distorting the octahedra the magnetic properties are substantially changed. In particular, decreasing the $\text{Ni-O}_{\text{apex}}/\text{Ni-O}_{\text{planar}}$ ratio from 1.16 to 1.08 the moment in La_2NiO_4 increases rapidly to $1.2 \mu_B$. Moreover at a ratio of 1.08 the system goes through a metal-insulator transition (Figure 4). Decreasing this ratio further from 1.08 to 1.00 the moment slightly decreases because unoccupied La s/d states start crossing E_F . These states can be pushed up again across E_F by tilting the octahedra. That the magnetic and electronic properties are so sensitive to the distortions of the NiO_6 octahedra is because by changing the relative NiO bondlengths one changes the position of the d_{z^2} bands with respect to the $d_{x^2-y^2}$ bands. We find that at a ratio of 1.17 Ni minority d_{z^2} states are occupied and majority $d_{x^2-y^2}$ are unoccupied. By decreasing the bond length ratio the minority d_{z^2} are pushed up in energy. At a ratio of 1.08 all the minority d_{z^2} states are pushed through E_F and an energy gap between the majority and minority e_g bands opens up.

Table 3 The calculated local spin moment M_s (in μ_B) per formula unit in the antiferromagnetic La_2NiO_4 , versus its lattice constant a (in Å) for $\text{Ni-O}_{\text{apex}}/\text{Ni-O}_{\text{planar}} = 1.11$.

a	3.816	3.855*	3.894	3.932	3.971	4.009	4.048	4.086
M_s	0.696	0.732	0.844	0.914	1.018	1.088	1.138	1.159

*denotes the experimental lattice constant

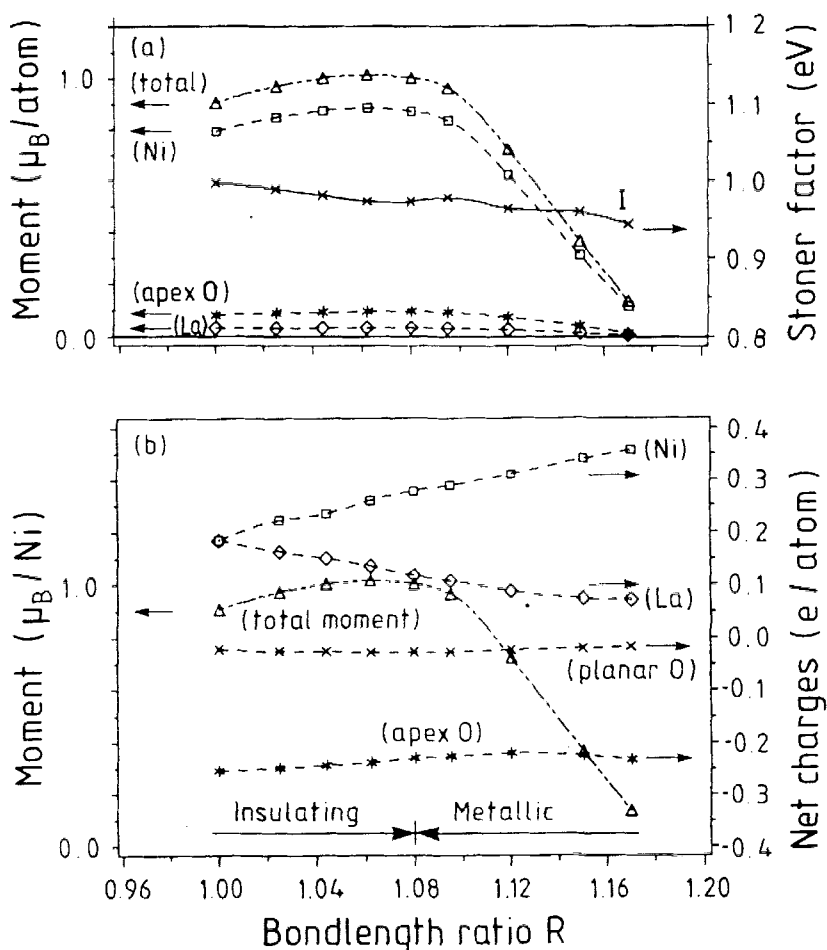


Figure 4 (a) Spin moment, site decompositions and Stoner factor I versus the $\text{Ni-O}_{\text{apex}}/\text{Ni-O}_{\text{planar}}$ bondlength ratio, and (b) net charges on various ions and total spin moment as a function of the $\text{Ni-O}_{\text{apex}}/\text{Ni-O}_{\text{planar}}$ bondlength ratio, in the antiferromagnetic and orthorhombic La_2NiO_4 .

5. CONCLUSIONS

With these improvements to the LMTO-ASA code, calculations for large unit cells can be performed reliably and accurately. Calculations for up to 56 atoms per unit cell were performed. For the antiferromagnetic calculations of La_2CuO_4 and La_2NiO_4 which have 14 atoms in the unit cell it took approximately 15 iterations to converge. Of course this number depends very much on the quality of the initial charge density used. We would use the converged charge density of a nearby lattice constant. Starting from 'scratch', i.e. suitable normalized atomic charge densities, would take at least double the amount of iterations. For La_2CuO_4 and La_2NiO_4 the Hamiltonian size was 154×154 and we took 150 k-point in the irreducible $1/8$ of the orthorhombic

Brillouin zone. These calculations, for 15 iterations, took 5 hours of Cray-XMP time. Figure 4 contains 9 such calculations and represents 50 hours of Cray-XMP. These calculations were multitasked. We used 3 tasks, each task solving the energy eigenvalue problem at a different k-point in the irreducible Brillouin Zone. This gave rise to 98% of parallelism.

The LSD seems to give a reasonable description of the electronic structure of La_2NiO_4 . There are several predictions from our calculations which could be verified by experimental studies. A possible implication of our results is that the LSD is valid for La_2NiO_4 , and the 'problem' with La_2CuO_4 would arise because of inaccuracies of the LSD and/or LMTO-ASA have the same energy value as the energy gain in finding the antiferromagnetic groundstate for La_2CuO_4 . This would mean that the oxygen holes would have $\text{pd } \sigma$ character, with twice as much planar O $p_{x,y}$ as apex O p_z .

Acknowledgement

We wish to thank W.E. Pickett for his help in the development of the total energy LMTO-ASA Code.

References

- [1] M. Causà, R. Dovesi, C. Roetti, E. Kotomin and V.R. Saunders, "A periodic ab initio Hartree-Fock calculation on Corundum", *Chem. Phys. Lett.*, **140**,120 (1987).
- [2] P. Hohenberg and W. Kohn, "Inhomogeneous electron gas", *Phys. Rev.*, **136**,B864 (1964).
- [3] W. Kohn and L.J. Sham, "Self-consistent equations including exchange and correlation effects", *Phys. Rev.*, **140**,A1133 (1965).
- [4] O.K. Andersen, "Linear methods in band theory", *Phys. Rev.*, **B12** 3060 (1975); O.K. Anderson, "Linear methods in band theory", in *The Electronic Structure of Complex Systems*, edited by P. Phariseau and W.M. Temmerman, NATO ASI Series Physics, **B113** (Plenum Press, 1984 11; O.K. Andersen, O. Jepsen and D. Glötzel, "Canonical description of the band structure of metals", *Highlights of Condensed Matter Theory*, edited by F. Bassani, F. Fumi and M.P. Tosi (North-Holland 1985).
- [5] H.L. Skriver, *The LMTO Method* (Springer-Verlag 1984).
- [6] G. Lehmann and M. Taut, "On the numerical calculation of the density of states and related properties", *Phys. Status Solidi*, **B54**,469 (1972).
- [7] O. Jepsen and O.K. Andersen, "The electronic structure of HCP ytterbium", *Solid State Commun.*, **9**,1763 (1971); O. Jepsen and O.K. Anderson, "No error in the tetrahedron integration scheme", *Phys. Rev.*, **B29**, 5965 (1984).
- [8] W. Pickett, "Pseudopotential methods in condensed matter applications", *Computer Physics Reports*, in press (1989).
- [9] D.G. Anderson, "Iterative procedures for nonlinear integral equations", *J. Assoc. Comput. Mach.*, **12**,547 (1965).
- [10] G.P. Srivastava, "Broyden's method for self-consistent field convergence acceleration", *J. Phys.*, **A17**,L317 (1984).
- [11] J.R. Chelikowsky and S.G. Louie, "First principles linear combination of atomic orbitals method for the cohesive and structural properties of solids. Application to diamond". *Phys. Rev.*, **B29**,3470 (1984).
- [12] Proceedings of the International Conference on High T_c Superconductors and Materials and Mechanism of Superconductivity, *Physica*, **153-155** (1988).
- [13] International Symposium on the Electronic Structure of High T_c Superconductors, Rome 5-7 October 1988, (Pergamon Press) in press.
- [14] N. Nucker, J. Fink, J.C. Fuggle, P.J. Durham and W.M. Temmerman, "Evidence for holes on oxygen in the high- T_c superconductors $\text{La}_{2-x}\text{Sr}_x\text{CuO}_4$ and $\text{YBa}_2\text{Cu}_3\text{O}_{7-y}$ ", *Phys. Rev.*, **B37**,5158 (1988).
- [15] N. Nucker, H. Romberg, X.X. Xi, J. Fink, B. Gegenheimer and Z.X. Zhao, "On the symmetry of holes in high- T_c superconductors", submitted to *Phys. Rev. B*.

- [16] P.A. Sterne, C.S. Wang, G.M. Stocks and W.M. Temmerman, "Electronic structure and antiferromagnetism in La_2CuO_4 ", *Mat. Res. Soc. Symp. Proc.*, **99**,353 (1988); P.A. Sterne and C.S. Wang, "Oxygen vacancies and antiferromagnetism in La_2CuO_4 ", *Phys. Rev.*, **B37**,7472 (1988).
- [17] G.Y. Guo, W.M. Temmerman and G.M. Stocks, "On the metal-semiconductor transition and antiferromagnetism in La_2CuO_4 ", *J. Phys. C: Solid State Phys.*, **21**,L103 (1988).
- [18] W.M. Temmerman, Z. Szotek and G.Y. Guo, "A local spin density study of antiferromagnetism in La_2CuO_4 and $\text{YBa}_2\text{Cu}_3\text{O}_6$ ", *J. Phys. C: Solid State Phys.*, **21**,L867 (1988).
- [19] G.Y. Guo and W.M. Temmerman, "Electronic structure and magnetism in La_2NiO_4 ", *Phys. C: Solid State Phys.*, **21**,L803 (1988).
- [20] G.Y. Guo and W.M. Temmerman, "On the electronic and magnetic properties of La_2NiO_4 : The importance of La-O planes", submitted for publication.
- [21] U. vonBarth and L. Hedin, "A local exchange-correlation potential for the spin polarized case: I", *J. Phys. C: Solid State Phys.*, **5**,1629 (1972).